

## Performance analysis of non-circular microchannels flooded with CuO-water nanofluid

Rajesh GAUTAM<sup>1</sup>, Avdhesh K. SHARMA<sup>2</sup>, Kapil D. GUPTA<sup>3</sup>

\*Corresponding author: Tel.: ++11 (0)9416722212; Fax: ++11 (0)1302484004; Email: avdhesh\_sharma35@yahoo.co.in

1: PDM, Bahadurgarh, Haryana, INDIA

2 & 3: Deenbandhu Chhotu Ram University of Science & Technology, Murthal, Sonapat, Haryana, INDIA

**Abstract** In this study the performances of various non-circular microchannel heat sinks (normalized with circular shape) have been comparatively analyzed for CuO-water nanofluid and baseline pure water flow. Nusselt number and Poiseuille number for each microchannel and thermo-physical properties of CuO-water nanofluid (viz., thermal conductivity, viscosity, specific heat and density) have been designed either empirically or from literature. Results for trapezoidal shape gives highest normalized pressure drops among all cases. Thermal performances for constant heat flux and constant wall temperature boundary conditions have been assessed in terms of normalized outlet wall temperature and normalized heat exchange rate. Results show that when thermal performance of any microchannel heat sink (MHS) improves, the hydraulic performance deteriorates. Trapezoidal microchannel gives best thermal performance in terms of normalized heat exchange rate specially with CuO-water nanofluids flow.

**Keywords:** CuO-water nanofluids, microchannels, effective thermal conductivity, hydraulic performance

### 1. Introduction

Faster cooling is crucial for development of smaller and compact microscale devices (i.e., microchannels heat sinks). It is well known that solid metals have orders-of-magnitude larger thermal conductivities than liquids. Thus any addition of metallic particles either of microscale or nanoscale may alter the thermo-physical properties (viz., thermal conductivity, viscosity, specific heat and density) of resulting fluid. The addition of microscale particle is not a practical proposition, as it shows poor suspensions characteristics (unstable), while nanoscale particles shows wonderful suspension characteristics leading to higher heat transfer. Furthermore, the recent advancement in nanotechnology has made it possible to produce nanometer-sizes particles using inert-gas condensation, mechanical grinding process, chemical vapor deposition, chemical precipitation, micro emulsions, thermal spray, and spray pyrolysis. Eastman et al (1996), have revealed that these nanosize particles (size of less than 100 nm and are oxides of high thermal conductive metals such as CuO,

Al<sub>2</sub>O<sub>3</sub> etc.) can have stable suspension in industrial heat transfer fluids (i.e. water, ethylene glycol, engine oil) that results in a new class of coolants. These advanced fluids enable to solve the problems such as sedimentation, clogging, settling of solid-particles, scaling and erosions. The increased interest in microchannels is due to advance manufacturing technologies (etching, vapour deposition, diffusion bonding, extruded aluminum multichannel tubes,...), which made it possible to construct microchannels in the range of 1  $\mu$ m - 1 mm. These microchannels are most effective for high-flux heat transfer technologies to provide extremely high heat transfer rates. The application of nanofluids in microchannels can augment the heat transfer rates further (due to both the high thermal conductivity and convective heat transfer coefficient) but at the expense of high pressure drops; it is due to higher values of viscosities of nanofluids.

Considerable works have been reported in past on production and properties of nanofluids (Keblinski et al 2008, Lee et al 1999, Koo and Kleninstreuer 2004, Jang and Choi 2007, Vajjha and Das 2009, Sharma and

Singh 2008). Researchers have improved the formulation for effective thermal conductivity of nanofluids by accounting either the influence of Brownian motion (Lee et al 1999, Koo and Kleninstreuer 2004, Vajjha and Das 2009) or the effect of particle aggregation and interfacial nanolayer (Murshed et al 2008). Koo and Kleinstruer (2004) proposed that effective thermal conductivity for concentration range of  $1\% < \phi < 4\%$  is composed of the combination of static and Brownian motion part. Later, Vajjha and Das (2009) improved the model by broad range of  $1\% < \phi < 6-10\%$  for three nanofluids. While the effective thermal conductivity has received much attention in past, studies on effective viscosity, which influences the fluidity, is relatively less and diverged. However, Masuda et al (2008) and Nguyen et al (2007) have measured the dynamic viscosity of several water based nanofluids for temperatures ranging from room temperature to approximately  $70^{\circ}\text{C}$ . Nguyen et al reported the most complete experimental studies on dynamic viscosities using three cases of water-based nanofluids:  $\text{Al}_2\text{O}_3$ -water with 36 nm and 47 nm particles, and  $\text{CuO}$ -water with 29 nm particles. They varied fluid temperature from ambient to  $70^{\circ}\text{C}$ . Koo and Kleinstreuer (2005) investigated laminar nanofluid flow in micro heat-sinks using the effective nanofluid thermal conductivity model they had established. For the effective viscosity due to micro-mixing in suspensions, they proposed the impact of volume fraction of  $\text{CuO}$ -nanoparticles in laminar flow of water and ethylene glycol on the microchannel pressure gradient, temperature profile and Nusselt number (Nu). They recommended the use of high Prandtl number (Pr) carrier fluids, high aspect ratio channels, high thermal conductivity nanoparticles and treatment of channel surface to avoid nanoparticles accumulation.

Numerous works on single phase flow through microchannels have been reported in past (Warrier et al. 2002, Morini 2004, Liu and Garimella 2005), the work reported on nanofluid flow through microchannels is

relatively limited. Liu and Garimella (2005) presented interesting comparative study based on five approximate analytical models to predict convective heat transfer for rectangular microchannel heat sinks. An optimization procedure is developed based on minimization of the thermal resistance. Hasan et al. (2009) have performed numerical simulation on different circular/non-circular microchannel heat exchanger geometries to study the effect of size and shape of channels on the thermal and hydraulic performance. Kakac and Pramuanjaroenkij (2009) in his review reported convective heat transfer enhancement with nanofluid. Li and Kleinstruer (2008) analytically calculate the effect of nanoparticles flow in trapezoidal microchannel geometry on the pressure drop and Nusselt number. They observed enhancement in thermal performance of nanoparticle mixture flow with small increase in pumping power. Wen and Ding (2004) presented experimental study on convective heat transfer of  $\text{Al}_2\text{O}_3$ -deionized water nanofluid flowing through a copper tube.

From the literature survey it can be revealed that efforts were carried out towards enhancement of thermal conductivity (by using nanofluids) and convective heat transfer coefficient for individual microchannels either having triangular, square or rectangular... shape. A very few work is focused on microchannels flooded with water based nanofluids. Another hand, the thermal advantage earned due to nanofluid operated microchannel gives higher skin friction and hence demands more pumping power (or killing this thermal gain). As surface/volume ratio is very large, surface dominant factors become more important. Thus, a comparative study to investigate the geometry effect on circular/non-circular microchannels heat sinks on a common platform is needed. In the present work, therefore, the thermal and hydraulic performance of various non-circular microchannel heat sinks has been studied for the comparative analysis.

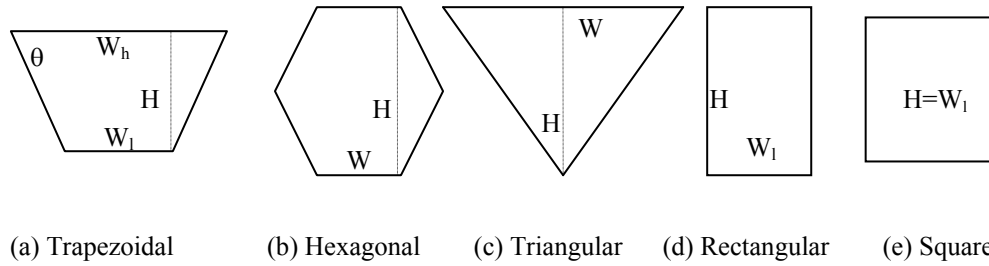


**Fig. 1 Non-circular shapes**

## 2. Formulation

For present study the thermal and hydraulic performance of various non-circular microchannel heat sinks designed for various shapes viz., trapezoidal and hexagonal, triangular, rectangular and square (refer fig. 1) has been evaluated. For known values of cross-sectional area ( $A_c$ ), microchannel channel length and shape of each microchannel; the perimeter and hydraulic diameter of each shape can be obtained easily as

### 2.1 Hydraulic diameter and shape factor

For a non-circular microchannel shapes (viz., trapezoidal and hexagonal, triangular, rectangular and square), the hydraulic diameter  $D_h$  can be defined in terms of cross-sectional area,  $A_c$ , and perimeter,  $p_j$ , as

$$D_{h,j} = \frac{4A_c}{P_j} \quad (1)$$

The perimeter of various microchannels can be written as

$$p_j = f(shape, A_c) \quad (2)$$

Here subscript  $j$  designate to circular, triangular, rectangular, square, trapezoidal and hexagonal shapes respectively.

### 2.2 Hydraulic Performance

The hydraulic performance of microchannel in each case can be presented in terms of pressure drop. For given Reynolds number ( $Re$ ), the pressure drop through the microchannel can be written following Judy et al (2002) as

$$\Delta P_j = \left( K_{ent} + \frac{f_j L}{D_h} + K_{dev} \right) \rho \frac{V_b^2}{2} \quad (3)$$

Where  $V_b = \mu_{eff} Re_{Dh} / \rho_{eff} D_h$  and  $K$  is the

pressure drop parameters and subscripts ent and dev corresponds to entrance and developing flow, respectively. In the present work, the effect of developing flow has been neglected.  $f$  is the friction factor for  $j^{th}$  microchannel, which can be calculated in terms of Poiseuille number ( $f_j = Po_j / Re_{Dh}$ ).  $Re_{Dh}$  can be defined ( $= \rho_{eff} V_b D_h / \mu_{eff}$ ) in terms of effective transport properties.

### 2.3 Thermal Performance

Circular/non-circular microchannel heat sinks were exposed to constant heat flux and constant wall temperature conditions for evaluating their thermal performances.

#### 2.3.1 Constant heat flux

Thermal performance of non-circular microchannel heat sinks with constant heat flux condition has been predicted in terms of outlet wall temperature of the microchannel. Thus, heat transport can be written as

$$\dot{Q}_j = \rho_{eff} V_b A_c C p_{eff} (Tb_o - Tb_i) \quad (4)$$

Here  $Tb$  is the bulk temperature and their subscripts  $i$  and  $o$  denote the inlet and outlet conditions.

The wall temperature at the outlet of each microchannel can be calculated holding energy balance in radial direction in terms of outlet bulk temperature and wall temperature, and convective heat transfer coefficient as

$$T_{w_o} = \frac{q''}{h_j} + Tb_o \quad (5)$$

Convective heat transfer coefficient for each microchannel is written as

$$h_j = \frac{k_{eff} Nu_j}{D_{h,j}} \quad (6)$$

### 2.3.2 Constant wall temperature

The thermal performance of circular/non-circular microchannel for constant wall temperature can be predicted in terms of heat transfer rate. The temperature profile through each microchannel can be written as

$$\frac{T_w - T_{b_o}}{T_w - T_{b_i}} = e^{-\frac{P_j L}{\rho_{eff} V_b A_c C p_{eff}} h_j} \quad (7)$$

Here,  $h_j$  is the convective heat transfer coefficient, which can be defined by eqn. (6)

The heat exchange rate in each microchannel can be simplified as

$$\dot{Q}_j = \rho_{eff} V_b A_c C p_{eff} (T_w - T_{b_i}) \left[ 1 - e^{-\frac{P_j L}{\rho_{eff} V_b A_c C p_{eff}} h_j} \right] \quad (8)$$

### 2.3.3 CuO-water Nanofluid flow

Thermal performance of microchannel heat sinks with nanofluids flow either in constant heat flux condition or constant wall temperature conditions cannot be predicted using the conventional expressions for Nu (as applicable for pure water flow). Therefore, for accounting the effect of concentration of CuO nanoparticles, one more term relating to volumetric nanoparticle concentration, Reynolds number, Prandtl number and particle Peclet number is needed. Chein and Huang (2005) have already reported such expression. Therefore, the same has been adapted in this work in following form

$$Nu_{NF} = Nu_{PWF} + 4.88\phi^{0.754} Pe_d^{0.218} Re^{1/3} Pr^{0.4} \quad (9)$$

Here Peclet number  $Pe_d$  and Prandtl number  $Pr$  are defined as

$$Pe_d = \frac{u_b d_p}{\alpha_{eff}} \quad \text{and} \quad Pr = \frac{\mu_{eff}}{\rho_{eff} \alpha_{eff}} \quad (10)$$

Where thermal diffusivity can be defined as

$$\alpha_{eff} = \frac{k_{eff}}{(\rho.Cp)_{eff}} \quad (11)$$

The properties of CuO-water nanofluid i.e., viscosity, thermal conductivity, specific heat and density are calculated from different sources as described below.

## 2.4 Properties of CuO-water nanofluid

### 2.4.1 Effective specific heat and density

The effective specific heat of nanofluids can be obtained from the relation of Xuan and

Roetzel (2000), which is based on thermal equilibrium of solid nanoparticles and liquid phase as

$$(\rho Cp)_{eff} = (1-\phi)(\rho Cp)_{bf} + \phi(\rho Cp)_p \quad (12)$$

The density of nanofluids is calculated using the liquid-particle mixture theory as

$$\rho_{eff} = \phi.\rho_p + (1-\phi).\rho_{bf} \quad (13)$$

### 2.4.2 Effective thermal conductivity

Since, thermal conductivity of solid metals are much higher than fluids, the high nanoparticle concentration in base fluid (i.e. nanofluids) enables enhancement in thermal conductivity value. There is experimental evidence that enhancement is much higher than the expectations. The thermal conductivity of nanofluids depends on concentration of nanoparticles, its thermal conductivity and their size, and thermo-physical properties of carrier-fluid. For this analysis, thermal conductivity of nanofluids is computed using the models of Koo and Kleinstreuer (2005), and Vajjha and Das (2009). It describes the thermal conductivity in terms of particle's conventional static and Brownian motion contribution. The static part is expressed as

$$\frac{k_{static}}{k_{bf}} = \frac{k_p + 2k_{bf} - 2(k_{bf} - k_p)\phi}{k_p + 2k_{bf} + (k_{bf} - k_p)\phi} k_{bf} \quad (14)$$

While, Brownian contribution is written as

$$k_{brownian} = 5 \times 10^4 \beta \phi \rho_{bf} C p_{bf} f \sqrt{\frac{k_b T}{\rho_p d_p}} \quad (15)$$

Where  $\beta$  and  $f$  were introduced to consider the hydraulic interaction among the Brownian motion induced fluid parcels and the particle interaction due to the particle interaction potential to encapsulate the strong temperature dependence for CuO-water nanofluid in the range of  $1\% \leq \phi \leq 6\%$  and  $298 \leq T \leq 363$  K (Vajjha and Das 2009)

$$\beta = 9.881(100\phi)^{-0.9446} \quad (16)$$

$$f = (2.8217 \times 10^{-2} \phi + 3.917 \times 10^{-3}) \left( \frac{T}{273} \right) - (3.0669 \times 10^{-2} \phi + 3.91123 \times 10^{-3}) \quad (17)$$

Thus, the effective thermal conductivity of the nanofluid ( $k_{eff}$ ) can be obtained by combining the conventional static part (based on Maxwells Model) and Brownian motion contribution as

$$k_{eff} = k_{static} + k_{brownian} \quad (18)$$

### 2.4.3 Effective Viscosity:

For the present analysis, a theoretical or empirical correlation for viscosity of CuO-water nanofluid is required that can reflect the effect of particle size, volume fraction and temperature. In fact, a very few experimental data on viscosity for CuO-water nanofluid, is available in the open literature which show diverging trends. Therefore, in the present work, a reliable experimental data of Nguyen et al (2007) for CuO-water nanofluid with particle diameter of 29 nm, has been used to correlate the effective viscosity in terms of fluid temperature and particle volume concentration as

$$\mu_{eff} = 0.147248 + \frac{19.5}{T} + 0.0223125\phi^2 + \frac{11.06}{T^2} + 8.4517557 \frac{\phi}{T^2} \quad (19)$$

Since the values of constants in eqn. (19) are derived empirically, the validity of the above expression is limited within the temperature range of 20-58.7°C and particle volume concentration range of 0-9%, respectively. Predicted data are found within the maximum error range of  $\pm 5\%$ .

The viscosity of base fluid (i.e., distilled water) is obtained following the expression as reported by Nguyen et al (2007)

$$\mu_{bf} = 10^{-7} \times e^{\frac{1.12646 - 0.039638T}{1 - 0.00729769T}} \quad (20)$$

## 3. Results and discussion

The hydraulic and thermal performance of various non-circular microchannel heat sinks for constant heat flux and constant wall temperature conditions and flooded with CuO-water nanofluid, have been normalized with circular geometry for better correspondence of results. Performance is presented based on single channel. Thermal performance of circular/non-circular microchannel heat sink for constant heat flux and constant wall temperature condition is presented in terms of normalized heat exchange rate and normalized outlet wall temperature through the microchannel, which is normalized by dividing by the result of circular microchannel. The flow through the microchannel is studied in laminar regime (400-1600) with fully

developed flow (i.e., thermally as well as hydraulically). The properties of working fluid are assumed to be constant. The cross-section area and length of microchannel are fixed at 27 mm and  $4.28 \times 10^{-8} \text{ m}^2$  respectively.

### 3.1 Hydraulic performance

The hydraulic performance of different microchannel geometry (viz. triangular, rectangular, square and hexagonal) is obtained in normalized form of pressure drop with circular geometry.

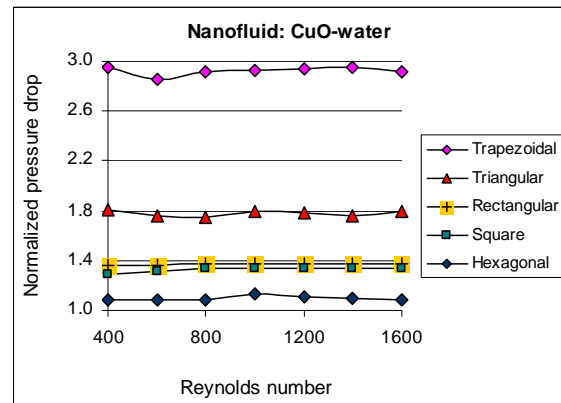


Fig. 2 Effect of geometry on normalized pressure drop (CuO-water nanofluid).

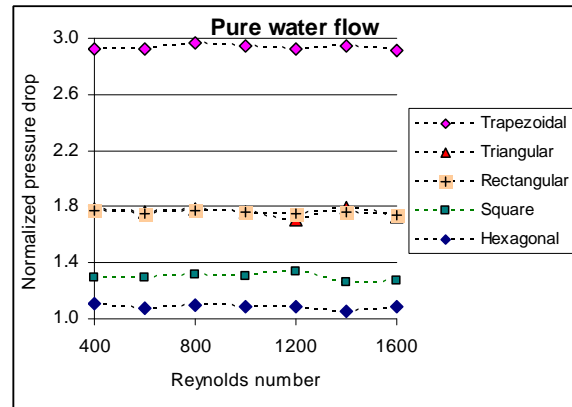


Fig. 3 Effect of non-circular geometries on normalized pressure drop for pure water flow.

The trends of normalized pressure drops through non-circular microchannel for pure water flow and CuO-water nanofluid flow are plotted against Reynolds number in figs. 2-3. From both cases, it is clear that normalized pressure drop in each microchannel geometry is not sensitive to Reynolds number. It should be noted here that the pressure drop through each microchannel is sensitive to Reynolds number. Furthermore, trapezoidal geometry

gives the highest value, while hexagonal shape gives lowest value of normalized pressure drop trends for both pure water as well as CuO-water nanofluid flow. It is also observed that nanofluid offers more resistance to flow through the microchannels of any shape. It is expected due to higher viscosity values of CuO-water nanofluid specially at higher particle concentrations.

### 3.2 Thermal performance

In this section, the thermal characteristics of microchannel using pure water and nanofluid flow (CuO-water) were studied in laminar regime. The characteristics of microchannels (except trapezoidal) were studied for two different boundary conditions, namely constant wall temperature and constant heat flux. The inlet temperature of cold streams for all cases is kept constant at 20°C.

#### 3.2.1 Constant Heat flux

For constant heat flux condition, the thermal performance of non-circular microchannel heat sinks were evaluated in terms of outlet wall temperature, which is normalized with circular geometry and referred as normalized outlet wall temperature in subsequent discussions. At this end, a constant heat flux of 431.47kW/m<sup>2</sup> is supplied externally to each microchannel heat sinks following Li et al, (2008). The cases for triangular, rectangular, square and hexagonal microchannel shapes have been simulated. The influence on normalized outlet wall temperature each microchannel against Reynolds number is compared for baseline pure water flow and CuO-water nanofluid flow as shown in fig. 4-5.

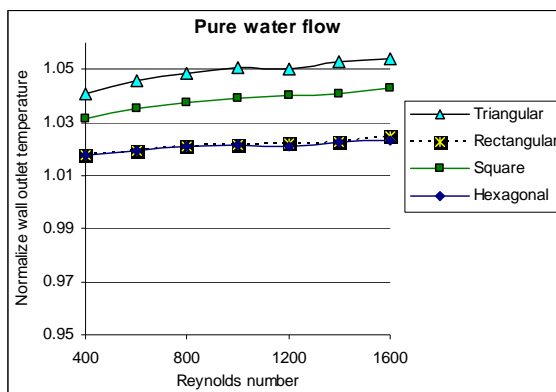


Fig. 4 Effect of non-circular shapes (for pure

water flow) on the normalized outlet wall temperature for constant heat flux condition.

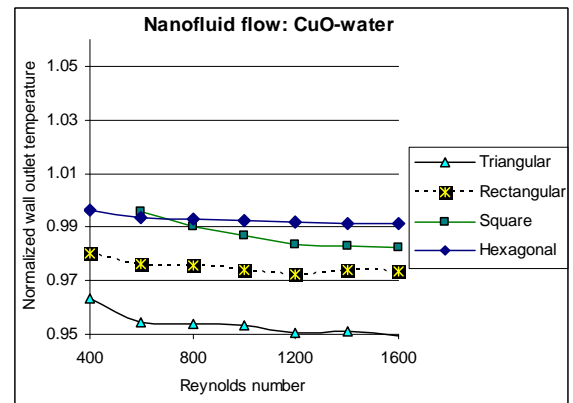


Fig. 5 Effect of non-circular shapes (for CuO-water nanofluid flow) on normalized outlet wall temperature for constant heat flux conditions.

The results of pure water flow (refer fig. 4) show that normalized outlet wall temperature of microchannel heat sinks increases with Re. For triangular microchannel, the highest value of normalized outlet wall temperature is observed, while for hexagonal and rectangular cases, there are lowest trends. Unlike pure water flow, the normalized outlet wall temperature for CuO-water nanofluid flow decreases with Re. Triangular microchannel gives lowest values of normalized outlet wall temperature, while hexagonal shape tends to highest (refer fig. 5). The lowest value of normalized outlet wall temperature in case of triangular shape is expected. For constant heat flux, the perimeter of triangular microchannel is highest while hydraulic diameter is lowest (cf. table 1) which gives high heat transfer coefficient for nanofluids flow. The variation of wall temperatures among the microchannel is found to be relatively small in contrast to pure water flow. It may be expected due to significant role of nanoparticle concentration on convective heat transfer.

Table 1. Perimeter and Hydraulic diameter of different Geometries



Geometry	$P_i$ (mm)	$D_h$ (mm)
Circle	0.734	0.234
Triangular	0.944	0.182
Square	0.828	0.207
Rectangle	0.837	0.205
Trapezoidal	0.110	0.156
Hexagonal	0.770	0.223

### 3.2.2 Constant wall temperature

For this case, thermal performance of the microchannel heat sinks is assessed in terms of the heat exchange rate, which is normalized by baseline circular shape. The wall temperature of microchannel has been fixed at 70°C. Fig. 6 for pure water flow reveals that normalized heat exchange rate improves marginally with Reynolds number for these shapes. Among all cases, the trapezoidal microchannel is found to be marginally sensitive with Reynolds number and also shows highest normalized heat exchange rate, while hexagonal microchannel gives the lowest value with pure water flow.

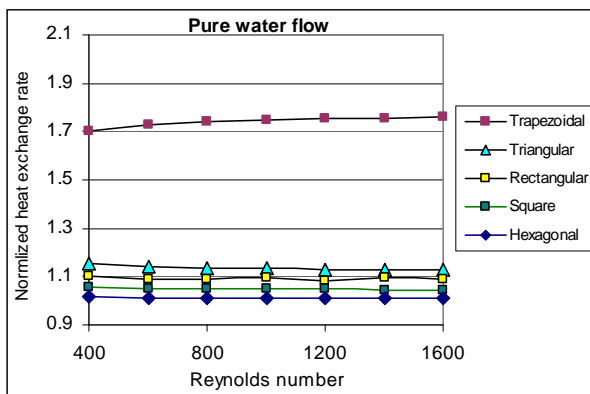


Fig. 6 Effect of non-circular shapes (for pure water flow) on the normalized heat exchanged rate at constant wall temperature.

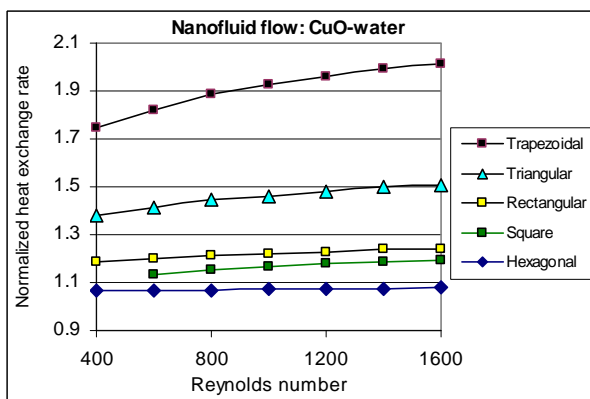


Fig. 7 Effect of non-circular shapes (for CuO-

water nanofluid) on the normalized heat exchanged rate at constant wall temperature.

Fig. 7 gives the influence of variation in Reynolds number on normalized heat exchange rate with CuO-water nanofluid at volumetric concentration of 4%. The case of trapezoidal microchannel shows strong function of normalized heat exchange rate, while hexagonal geometry gives lowest value showing hardly any relation with Reynolds number.

For trapezoidal microchannel, the hydraulic diameter is minimum, thus heat transfer must be maximum for both pure water and CuO-water nanofluid. Furthermore, Nu for rectangular shape microchannel is higher than that of triangular shape leading to high heat transfer. Moreover, for CuO-water nanofluid, the Nu for both the cases (rectangular and triangular) become marginal, and heat transfer coefficient for convection strongly dominated by hydraulic diameter (refer eqn. 1). Since the hydraulic diameter of the triangular case is less than that of rectangular, the heat exchange rate of triangular microchannel will be much higher than that of rectangular microchannel.

## 4. Conclusion

Hydraulic and thermal performances (normalized with circular geometry) of non-circular microchannel heat sinks have been compared for pure water flow and CuO-water nanofluid flow. Results of normalized pressure drop through trapezoidal microchannel for pure water and CuO-water nanofluid flow for constant heat flux are found to be sensitive with Reynolds number. For constant heat flux, normalized wall temperature is found to be decreased with Reynolds number for cases investigated (except trapezoidal shape). These results are more sensitive for nanofluid flow. Moreover, triangular shape gives lowest trends allowing scope for more heat transport. For pure water flow, the trends are just opposite.

For constant wall temperature, in pure water flow, trapezoidal channel shows clear domination for normalized heat exchange rate, while hexagonal shape gives lowest trends for

same Reynolds number range. When thermal performance of microchannel heat sink improves, the hydraulic performance deteriorates and vice versa. Therefore, the thermal and hydraulic performance of trapezoidal microchannel heat sink must be optimized to develop advance Microscale cooling devices for current and future heat removal applications

## References

- Chein R., Huang G., 2005. Analysis of microchannel heat sink performance using nanofluids. *Applied Thermal Engg.*; 25, 3104-14.
- Eastman J.A., Choi U.S., Lee S., Topson L.J., Lee A.S., 1996. Enhanced Thermal Conductivity through the development of nanofluids. Conference: 1996 Fall meeting of the Materials Research Society (MRS), Boston, MA (United States), 2-6 Dec 1996.
- Hasan M.I., Rageb A.A., Yaghoubi M., Homayoni H., 2009. Influence of channel geometry on the performance of a counter flow microchannel heat exchanger. *Int. J. of Thermal Sciences*, 48, 1607-18.
- Jang S.P., Choi S.U.S., 2007. Effect of various parameters on nanofluids thermal conductivity. *J. of Heat Transfer*, 129, 617-23.
- Judy J., Maynes D., Webb B.W., 2002. Characterization of frictional pressure drop for liquid flows through microchannels. *Int. J. of Heat and Mass Transfer*; 45, 3477-89.
- Kakac S., Pramuanjaroenkij A., 2009. Review of convective heat transfer enhancement with nanofluids, *Int. J. of Heat and Mass Transfer*, 52, 3187-96
- Keblinski P., Prasher R., Eapen J., 2008. Thermal conductance of nanofluids: is the controversy over? *J. of Nanoparticles Research*, 10, 1089-97.
- Koo J. and Kleinstreuer C., 2004. A new thermal conductive model for nanofluids. *J. of Nanoparticles Research*, 6, 577-88.
- Koo, J. Kleinstreuer C., 2005. Laminar nanofluid flow in microsheet-shinks. *Int. J. Nanoparticle Res.*, 48, 2652-61.
- Lee S., Choi S.U.S., Li S., Eastman J.A., 1999. 'Measuring thermal conductivity of fluids containing oxide nanoparticles'. *Journal of Heat Transfer*, 121, 280-88.
- Li J., Kleinstreuer C., 2008. Thermal performance of nanofluids flow in microchannels. *Int. Journal of Heat and Fluid Flow*, 29, 1221-32.
- Liu D., Garimella S.V., 2005. Analysis and Optimization of the thermal performance of microchannel heat sinks. *Int. J. of Numerical Methods for Heat Fluid Flow*, 15, 7-26.
- Morini G.L., 2004. Single phase convective heat transfer in microchannels: a review of experimental results, *Int. J. of thermal sciences*, 43, 631-51.
- Murshed S.M.S, Leong K.C., Yang C., 2008, Investigation of thermal conductivity and viscosity of nanofluids. *Int. J. of Thermal Science*, 47, 560-68.
- Nguyen C.T., Desgranges F., Roy G., Gallanis N., Mare T., Boucher S., Mintsa H. A., 2007. Temperature and particle- size dependent viscosity data for water- based nanofluids- Hysteresis phenomenon. *Int. J. of Heat and Fluid Flow*, 28, 1492-506.
- Pak and Cho
- Sharma A.K., Singh A.K., 2008. Model development for effective thermal conductivity and dynamic viscosity of alumina-water nanofluids. *Proceeding of the 1<sup>st</sup> European conf. on Microfluidics*; pp. 1-10.
- Vajjha R.S., Das D.K., 2009. Experimental determination of thermal conductivity of three nanofluids and development of new correlation. *Int. J. of Heat & Mass transfer*, 4675-82.
- Warrier GR, Dhir VK, Mamoda LA, 2002. Heat transfer and pressure drop in narrow rectangular channels. *Exp. Thermal and Fluid Science*, 26, 53-64.
- Wen D., Ding Y., 2004. Experimental investigation into convective heat transfer of nanofluids at the entrance region under laminar flow conditions. *Int. J. of Heat and Mass Transfer*, 47, 5181-88.
- Xuan Y, Roetzel W., 2000. Conception for heat transfer correlation of nanofluids. *Int. J. Heat Mass Transfer*, 43, 3701-7.